Electrochemical Reduction of Carbon Dioxide on Cu/CuO Core/Shell Catalysts

Yangchun Lan,[a, b] Chao Gai,[c] Paul J. A. Kenis,*[b] and Jiaxing Lu*[a]

We investigate the electrochemical behavior of different loadings of a Cu(core)/CuO(shell) catalyst in a standard three-electrode cell, which reveals transformations between Cu, Cu^I, and CuO species. The electroreduction of CO_2 on the catalyst is performed in an aqueous solution within a flow reactor. CO and HCOOH are the main products, with H_2 as a byproduct. When the catalyst loading is 1.0 mg cm^{-2}, the faradaic efficiencies of CO and HCOOH are higher than those with other catalyst loadings, with a short reaction time. This paper also focuses on the experimental and kinetic details of the electroreduction process of CO_2 to CO and HCOOH when using the Cu/CuO catalyst. Reactions are modeled by using an in-series, first-order reaction, and the models are verified to reasonably describe the two products formed during the electroreduction of CO_2. According to the kinetic analysis, the rate constant for HCOOH production is higher than that of CO.

1. Introduction

Carbon dioxide (CO_2) is the most notorious greenhouse gas, which is released by both natural and artificial processes, leading to atmospheric CO_2 levels rising and contributing to global warming. One possibility is to trap CO_2 and to convert it into fuels and organic materials.[1, 2] Photochemical and electrochemical reductions of CO_2 are potential cost-effective processes for chemical production, which simultaneously take advantage of this sustainable energy source.[3] Electrochemical reduction of CO_2 has generated substantial interest as a potential method for producing valuable chemicals by using CO_2 as the sole carbon source. Potential products obtained from the electroreduction of CO_2 generally include CO, HCOOH, HCHO, CH_3OH, CH_4, and other hydrocarbons. The selectivity of CO_2 electroreduction depends heavily on the reaction conditions and the catalysts used.[4, 5]

 CO_2 is an abundant and potentially low-cost carbon source for the production of fuels and organic chemicals. However, a major hurdle in CO_2 reduction is the kinetic inertness of CO_2. The reduction of CO_2 to CO_2^- has a standard potential (E^o) of −1.9 V versus a normal hydrogen electrode (vs. NHE) at pH 7 in water.[6] Over the past three decades, researchers have utilized both homogeneous molecular catalysts[7, 8] and heterogeneous catalysts[9–11] to electrochemically reduce CO_2 in aqueous solutions, which could overcome kinetic barriers and poor stability. The Bocarsly group reported a system for electrochemical catalytic[7, 8] and photoelectrocatalytic[12] CO_2 reduction to HCOOH, HCHO, and CH_3OH, which used a homogeneous pyridinium catalyst. In 2011, Masel and co-workers used a flow reactor with silver nanoparticle catalysts suspended in an ionic liquid to electrochemically reduce CO_2.[13] This electrocatalytic system reduced CO_2 to CO at overpotentials below 0.2 V, and the faradaic efficiency was as high as 96%.

In heterogeneous catalysis, copper and copper oxide catalysts are capable of selectively producing hydrocarbons from CO_2, but are very inefficient, owing to high overpotentials. Recent literature reports,[9, 14–17] including those demonstrating the pathway for electrochemical reduction of CO_2 at a copper electrode based on density functional theory (DFT) and computational hydrogen electrode (CHE) models proposed by Peterson et al.,[18] confirmed that carbon monoxide is an important intermediate in the formation of hydrocarbons and alcohols. In the electroreduction process, the desired hydrogen evolution reaction competes with other reactions that produce undesired side products. Characterizing the electroreduction kinetics of all reactions, desired and undesired, will determine the undesired reactions that are the primary source of faradaic loss. Previous work has studied silver and gold nanoparticles as well as other transition-metal catalysts to produce CO and H_2 from CO_2.[19–22] Electroreduction of CO_2 on a catalyst with the same metal core/shell structure has not previously been reported. In this study, we investigated the electroreduction of CO_2 on different loadings of a Cu(core)/CuO(shell) catalyst in a flow reactor. Furthermore, we investigated the variation of electroreduction kinetics in the long-term reaction. These data

[a] Y. Lan, Prof. J. Lu
Key Laboratory of Green Chemistry and Chemical Process
Department of Chemistry, East China Normal University
Shanghai 200062 (PR China)
address:
E-mail: jxlu@chem.ecnu.edu.cn

[b] Y. Lan, Dr. P. J. A. Kenis
Department of Chemical and Biomolecular Engineering
University of Illinois at Urbana-Champaign
Urbana, IL 61801 (USA)
address:.
E-mail: kenis@illinois.edu

[c] Dr. C. Gai
Key Laboratory of High Efficiency and Clean Mechanical Manufacture
Department of Mechanical Engineering
Shandong University, Jinan 250061 (PR China)

provide a more in-depth understanding of the electroreduction of CO_2 in aqueous solutions.

Experimental Section

Cu(core)/CuO(shell) nanopowder (Alfa Aesar, APS 20–40 nm, 99.9%, metal basis) inks were prepared by mixing Millipore water (200 μL), the catalyst (4 mg), Nafion solution (5.2 μL, 5 wt%, Fuel Cell Earth), and isopropyl alcohol (200 μL, Fisher scientific, 99.9%). To fabricate the cathode for flow-reactor experiments, the mixed inks were subjected to sonication (Vibra-Cell ultrasonic processor, Sonics & Materials, Inc.) for 15 min and, then, they were hand-painted onto a microporous Sigracet 35 BC gas-diffusion layer (Ion Power, Inc.). The cathodes in the flow-reactor experiments were loaded with either 0.5, 1.0, 1.5, or 2.0 mg cm^{-2} Cu(core)/CuO(shell) catalyst on Sigracet 35 BC. However, all of the anodes (platinum black, Alfa Aesar, with a high surface area) used in the flow reactor were loaded with 1 mg cm^{-2} on the Sigracet 35 BC.

Electroanalytical experiments (Autolab potentiostat, PGSTAT-302N, EcoChemie) were conducted in 1 M KHCO$_3$ (Sigma Aldrich, Granular, ACS reagent, 99.7%). A standard three-electrode electrochemical cell was used, equipped with a glassy carbon electrode as the working electrode, a platinum gauze as the counter electrode, and a Ag/AgCl reference electrode in 3 M NaCl. All experiments were performed at 25 °C under atmospheric pressure. Catalyst inks were prepared by using the same method described above. The catalyst layer for the three-electrode-cell experiments was prepared by depositing a drop (5 μL) of the catalyst ink on a glassy carbon rotating-disk electrode (Metrohm 6.1204.300; polished with 0.05 μm alumina), which was dried under a flow of N$_2$.

The electroreduction in the flow reactor was performed at 25 °C under atmospheric pressure, and a Nafion 117 membrane was used to separate the cathode and anode compartments to prevent oxidation of the reduced CO_2 products. An Autolab potentiostat (Autolab PGSTAT-302N, EcoChemie), operating on chronoamperometric mode, measured the resulting current, as previously reported.[20] The individual electrode potentials were measured by using multimeter devices that were connected to each electrode and a Ag/AgCl reference electrode in the exit stream. A mass-flow controller (MASS-FLO, MKS instrument) was used to flow CO_2 from a cylinder at 7 sccm. 1 M KHCO$_3$ was injected into the flow reactor at 0.5 mL min^{-1} by using a syringe pump (PHD 2000, Harvard Apparatus). The cathode gas products were detected by using gas chromatography (Thermo Finnegan Trace GC), and the results were consistent with previously reported values.[19,21] Cathode liquid products were detected by a ^{1}H nuclear magnetic resonance (NMR) spectrometer (VARIAN UNITY INOVA 500, 500 MHz), and dimethylsulfoxide (DMSO, Fisher Scientific, 99.9%) was added to samples (1 mM final concentration) as an internal standard.[3,23] The water peak was suppressed by using a presaturation sequence. The NMR parameters were identical for all collected spectra, making standard curves to allow the quantification of products in the electrolyte. After each CO_2 reduction reaction, the electrolyte (200 μL) was mixed with 1 mM DMSO (100 μL) and D$_2$O (400 μL; Cambridge Isotope Laboratories, Inc., D 99.9%) for NMR analysis.

3. Results and Discussion

3.1. Cyclic Voltammetry

The electrochemical behavior of different loadings of a Cu-(core)/CuO(shell) catalyst was studied in a standard three-elec-

trode cell with 1 M KHCO$_3$ solution. As shown in Figure 1, the cyclic voltammograms for different catalyst loadings in the presence of Ar were similar to those in the presence of CO_2 after two continuous scans. Nevertheless, the first scan was clearly different from the second scan. In the first scan, in the presence of Ar (Figure 1 a1), the reduction peak (peak I) was close to −1.0 V, and the peak I current increased with increasing catalyst loadings. Peak I may be attributed to the reduction reaction of CuO to Cu, as the structure of the catalyst was core/shell. However, there were just two reduction peaks (peaks III and IV) located between −0.25 and −0.5 V in the second scan (Figure 1 a2). Two successive oxidation peaks (II) indicated transitions between the different valence states of copper, that is, Cu, Cu^I, and Cu^{II}. In general, the cyclic voltammetry results for Cu(core)/CuO(shell) indicated transformations between Cu, Cu^I, and Cu^{II}, which was in agreement with previous work.[24] When the 1 M KHCO$_3$ solution was saturated with CO_2 (Figures 1 b1 1 b2), the peak currents were much higher than under an Ar atmosphere when the catalyst loadings were between 0.5 and 1.5 mg cm^{-2}. After the CO_2 had dissolved into the solution, the CO_2 reacted with the catalyst or the protons at the surface of the electrode, leading to the current improved.[25] The current increased linearly with respect to catalyst loading.

3.2. Electrolysis

Chronoamperometric electrolysis was carried out in a divided flow reactor, equipped with gas-diffusion electrodes (GDEs), in the presence of CO_2 to further understand the effect of different Cu(core)/CuO(shell) catalyst loadings on the electroreduction of CO_2. Figure 2 shows the current density as a function of the cathode potential for different loadings of the catalyst (0.5, 1.0, 1.5, and 2.0 mg cm^{-2}. The current densities increased with increasing catalyst loading in the sequence 2.0 ≈ 1.5 > 1.0 > 0.5 mg cm^{-2}. At a cathode potential of −1.65 V versus Ag/AgCl, the current density observed for a catalyst loading of 2.0 mg cm^{-2} was approximately 65 mA cm^{-2}. These results supported the hypothesis that the conversion of CO_2 would be improved by increasing the catalyst loading from 0.5 to 2.0 mg cm^{-2}.[26]

The faradaic efficiency of CO_2 electroreduction, in a short reaction time, in 1 M KHCO$_3$ is shown in Figures 3a and b. The experimental results indicate that different catalyst loadings impact the faradaic efficiencies of CO and HCOOH, and that the electroreduction of CO_2 to CO on the Cu(core)/CuO(shell) catalyst occurs at a low overpotential (−1.2 V vs. Ag/AgCl). Specifically, the faradaic efficiency of CO when using a catalyst loading of 2.0 mg cm^{-2} was usually higher than the other catalyst loadings, whereas a reverse trend existed for HCOOH, which demonstrated that the faradaic efficiency could be higher at smaller catalyst loadings. However, by using the lower catalyst loading of 1.0 mg cm^{-2} at −1.78 V versus Ag/AgCl, the faradaic efficiency of HCOOH was highest with maximum value of about 20%, whereas the faradaic efficiency of CO was around 21%.
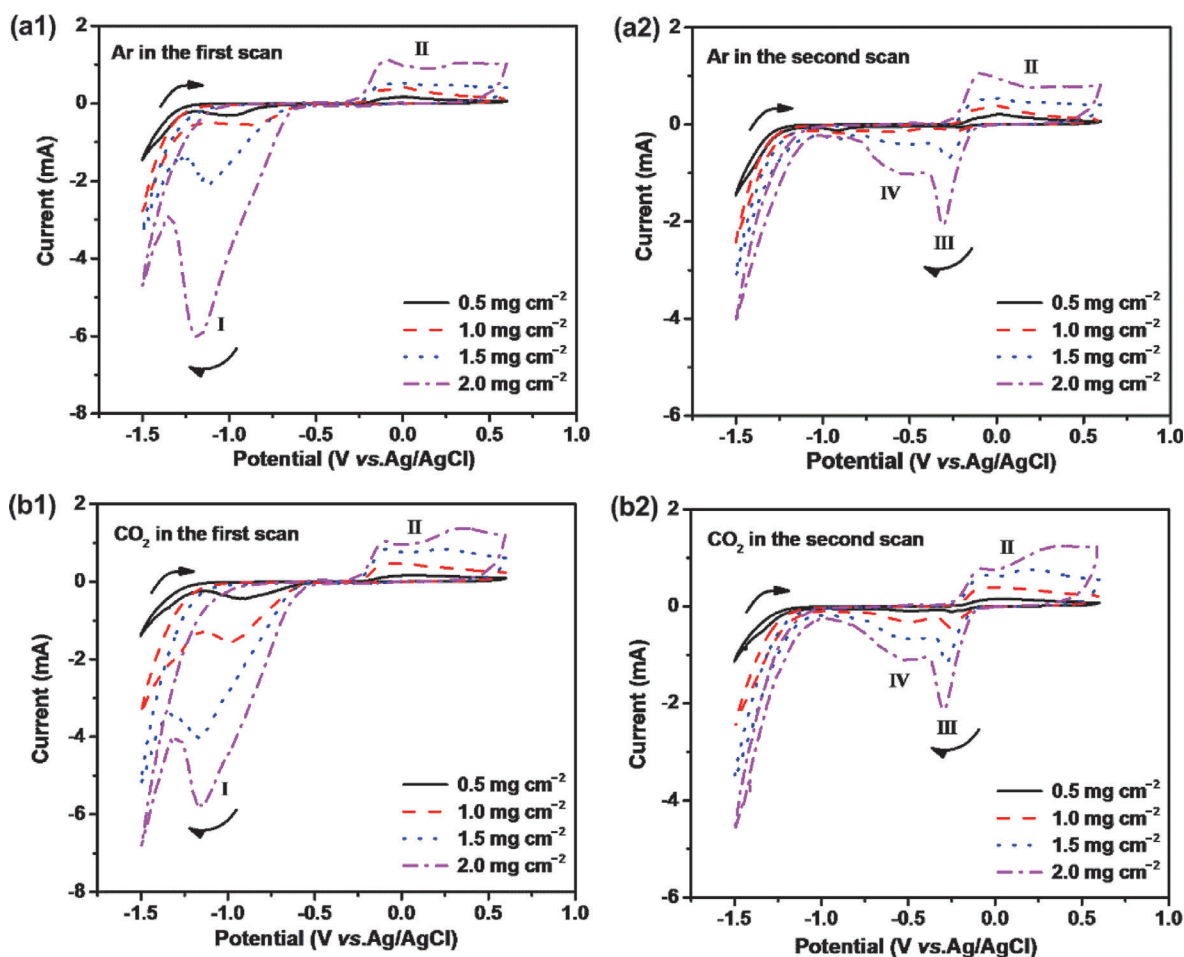
Figure 1. Cyclic voltammograms for the cathodes with different Cu(core)/CuO(shell) loadings in 1 м KHCO$_3$ and in the presence of Ar (a1, a2) and CO$_2$ (b1, b2). Scan rate = 0.1 V s^{-1}.
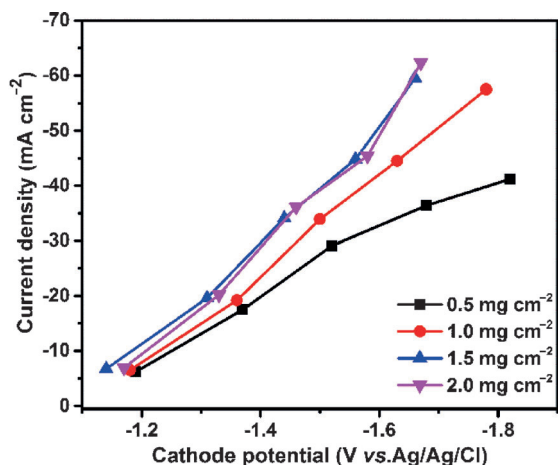

Figure 2. Effect of cathode potential and Cu(core)/CuO(shell) catalyst loading on the current density in a flow reactor

The effect of catalyst loadings on the partial current density of different products was also investigated. Plots of the partial current density versus the cathode potential for the production of CO and HCOOH are shown in Figures 3 a1 and b1. The values for the partial current density were produced by multi-

plying the current density (Figure 2) at a given potential by the faradaic efficiency. The partial current densities of CO and HCOOH always increased with increasing catalyst loadings. At −1.78 V versus Ag/AgCl, the partial current densities of CO and HCOOH were around 12 and 11 mA cm^{-2}, respectively, when the catalyst loading was 1 mg cm^{-2} and the current density was as high as 58 mA cm^{-2}. The result revealed that the selectivity towards both CO and HCOOH was almost the same during the electroreduction of CO$_2$ on the Cu(core)/CuO(shell) catalyst. Interestingly, some methanol (ca. 1–3 %) was also produced, indicating that the catalyst was capable of reducing CO$_2$ further.

3.3. Kinetic Analysis

Variations in the faradaic efficiencies and partial current densities for the products indicated that the two products have different reaction rates during the electroreduction of CO$_2$, also indicating that the multiple proton-coupled electron transfers to CO$_2$ were thermodynamically facile, which require a large overpotential even with the help of a catalyst.[8,27] Therefore, we investigated the electroreduction kinetics. The possible reaction pathway of the electrochemical reduction of CO$_2$ on the
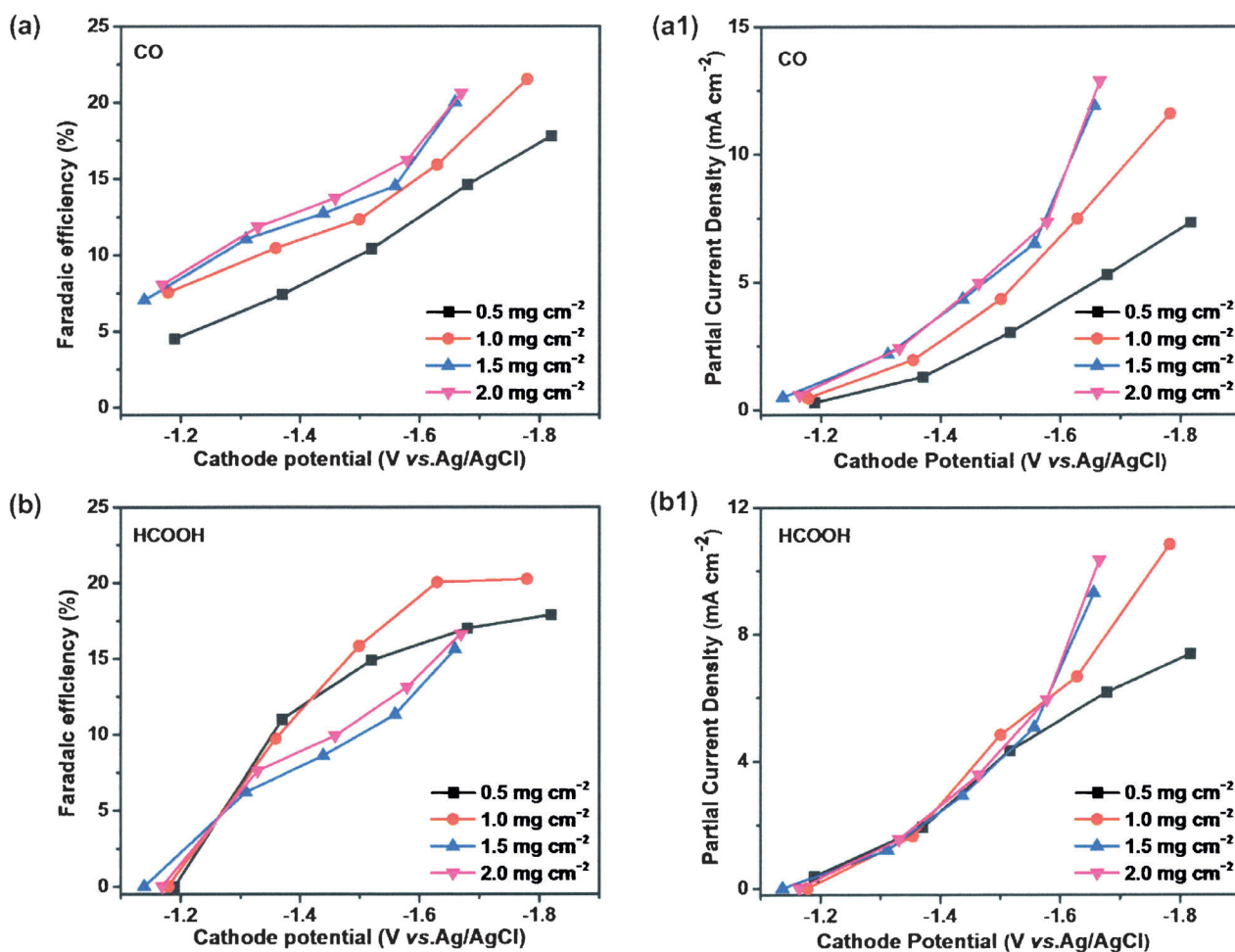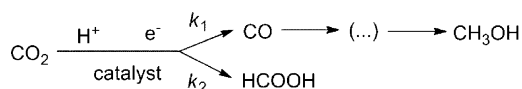
Figure 3. Faradaic efficiency of CO (a) and HCOOH (b) with different Cu(core)/CuO(shell) loadings in a flow reactor. Partial current densities of CO (a1) and HCOOH (b1) with different loadings of the Cu(core)/CuO(shell) catalyst.

Scheme 1. The possible reaction pathway for the electroreduction of carbon dioxide on a Cu(core)/CuO(shell) catalyst.

Cu(core)/CuO(shell) catalyst is proposed in Scheme 1. Competition existed between the two reactions.

The electroreduction process of CO_2 could be described by a series of first-order differential equations [Eqs. (1)–(3)]:[28]

$$-\frac{d[CO_2]}{dt} = \frac{d[CO]}{dt} + \frac{d[HCOOH]}{dt} + \ldots \ldots \tag{1}$$

$$\frac{d[CO]}{dt} = [CO]_0 e^{-k_1 t} \tag{2}$$

$$\frac{d[HCOOH]}{dt} = [HCOOH]_0 e^{-k_2 t} \tag{3}$$

where t is the reaction time and k_1 and k_2 are the reaction rate constants of CO and HCOOH, respectively. According to the long-term experimental results, the initial conditions are: $[CO_2]_0 = 3.12 \times 10^{-4}$ mol and $[CO]_0 = [HCOOH]_0 = 0$.

Comparison of the product formation profiles between the proposed first-order model and the experimental data are shown in Figure 4. The results indicate that the theoretical values of the moles of CO and HCOOH at different catalyst loadings are consistent with the experimental data. The model fits well with the experimental data, especially for CO. The results in Figure 4 illustrate that the predicted CO concentration increased in the first 20 min and then reached a constant value for the rest of reaction time, whereas the predicted HCOOH concentration increased quickly within a few minutes and then reached a constant value. Nevertheless, the measured amount of HCOOH increased sharply with an increase in the reaction time to 80 min, and then tended to decrease. Notably, when the catalyst loading was 1.5 mg cm^{-2}, the measured amounts of CO and HCOOH were higher than with other catalyst loadings with the long reaction time. The experimental results confirmed that the proposed mathematical model can predict the first-order model to a reasonable extent for the electroreduction of CO_2 to CO and HCCOH, and they show that an increase in reaction time could enhance the formation of the CO_2 reduction products.
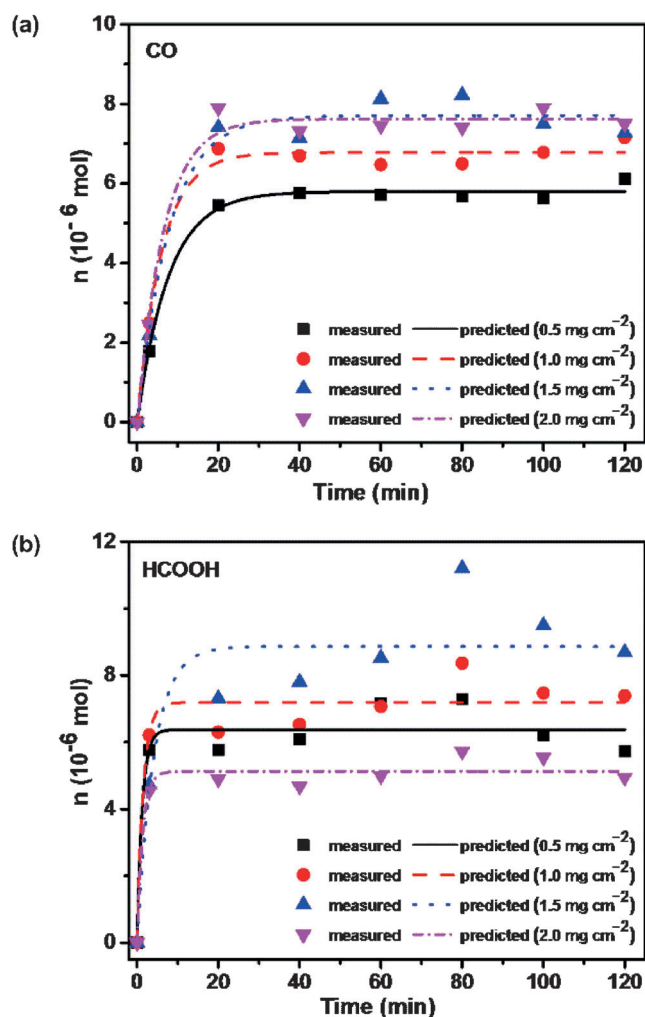
Figure 4. Comparison of the experimental results with the predicted values for CO (a) and HCOOH (b), based on differential first-order models. The lines are predicted based on a simulated first-order model and the dots represent the experimental data. Working electrode = Cu(core)/CuO(shell) catalyst on a GDE, counter electrode = Pt black loaded on a GDE, reference electrode = Ag/AgCl (3 M NaCl), electrolyte solution = 1 M $KHCO_3$, and temperature = 25 °C.

Figure 5 displays the rate constants for the two main products (CO and HCOOH) as a function of catalyst loading during the electroreduction of CO_2. The rate constants were calculated by using the first-order differential equations for k_1 and k_2, respectively. Notably, k_1 is smaller than k_2. A small rate constant indicates a lower reactivity. The small rate constant explains the low faradaic efficiency of CO compared with that of HCOOH during the long-term electroreduction process of CO_2 on the Cu(core)/CuO(shell) catalyst in this study. When increasing the catalyst loadings, the rate constants increased sharply; however, k_1 reached a constant and k_2 tended to decrease at 1.5 and 2.0 mg cm^{-2} loadings on the GDE. These changes suggest that the different Cu(core)/CuO(shell) catalyst loadings affected the rate of electroreduction of CO_2 in aqueous solution. The catalyst loading was 1.5 mg cm^{-2}, which aided the electrochemical reduction of CO_2 with the long reaction time.
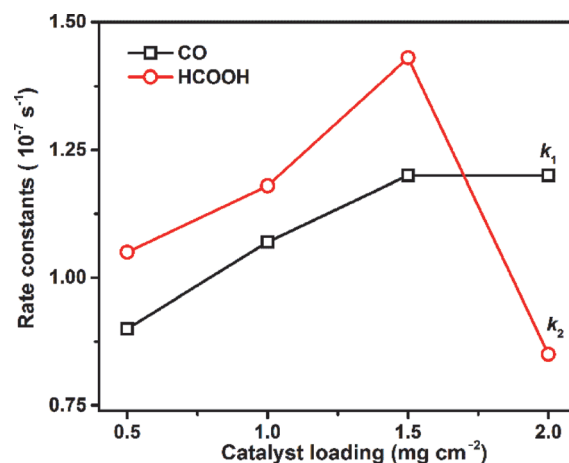

Figure 5. The rate constants k_1 and k_2 for CO and HCOOH, respectively, on a Cu(core)/CuO(shell) catalyst with different loadings, in a flow reactor and in the presence of 1 M $KHCO_3$.

4. Conclusions

A study of the electrochemical behavior of the Cu(core)/CuO(shell) catalyst in 1 M $KHCO_3$ revealed that the catalyst transformed between the various oxidation states of copper, namely Cu, and Cu^I, and Cu^{II}. The current peak intensity increased with increased catalyst loading. Chronoamperometric electrolysis was performed in a flow reactor to further investigate the effect of the catalyst loading on the process of CO_2 electroreduction. Faradaic efficiencies of CO and HCOOH were higher at a loading of 1.0 mg cm^{-2} on the GDE than with other catalyst loadings, when a short reaction time was used. Reactions were then modeled by using an in-series, first-order reaction, and the differential equations deduced from the models were compared to the experimental data. It was verified that the models could reasonably describe the evolution of products during the electroreduction of CO_2. Kinetic analysis indicated that the two products had different rate constants, leading to different reactivates and, therefore, different faradaic efficiencies. With a long reaction time, different catalyst loadings affected the rate of CO_2 electroreduction, and 1.5 mg cm^{-2} catalyst loading was favored for the electrochemical reduction of CO_2 to CO and HCOOH. Our results suggest that the interplay between the Cu core and the CuO shell is beneficial for the electroreduction of CO_2, but the catalyst requires further modification to suppress the pathways leading to other products, such as H_2.

[1] M. Aresta, A. Dibenedetto, *Dalton Trans.* **2007**, *28*, 2975–2992.

[2] C. S. Song, A. M. Gaffney, K. Fujimoto, *ACS Symp. Ser.* **2002**, *809*, 2–30.

[3] K. P. Kuhl, E. R. Cave, D. N. Abram, T. F. Jaramillo, *Energy Environ. Sci.* **2012**, *5*, 7050–7059.

[4] H. Yoneyama, *Catal. Today* **1997**, *39*, 169–175.

[5] R. P. S. Chaplin, A. A. Wrangg, *J. Appl. Electrochem.* **2003**, *33*, 1107–1123.

[6] Y. Oh, X. Hu, *Chem. Soc. Rev.* **2013**, *42*, 2253–2261.

[7] G. Seshadri, C. Lin, A. B. Bocarsly, *J. Electroanal. Chem.* **1994**, *372*, 145–150.

[8] E. Barton Cole, P. S. Lakkaraju, D. M. Rampulla, A. J. Morris, E. Abelev, A. B. Bocarsly, *J. Am. Chem. Soc.* **2010**, *132*, 11539–11551.

[9] Y. Hori, K. Kikuchi, S. Suzuki, *Chem. Lett.* **1985**, 1695–1689.

[10] Y. Hori, *Modern Aspects of Electrochemistry, vol. 42*, Springer, New York, **2008**, *42*, 89–189.

[11] Y. Chen, M. W. Kana, *J. Am. Chem. Soc.* **2012**, *134*, 1986–1989.

[12] E. E. Barton, D. M. Rampulla, A. B. Bocarsly, *J. Am. Chem. Soc.* **2008**, *130*, 6342–6344.

[13] B. A. Rosen, A. Salehi-Khojin, M. R. Thorson, W. Zhu, D. T. Whipple, P. J. A. Kenis, R. Masel, *Science* **2011**, *334*, 643–644.

[14] Y. Hori, A. Murata, T. Tsukamoto, H. Wakebe, O. Koga, H. Yamazaki, *Electrochim. Acta* **1994**, *39*, 1833–1839.

[15] M. Gattrell, N. Gupta, A. Co, *J. Electroanal. Chem.* **2006**, *594*, 1–19.

[16] S. Kaneco, K. Iiba, H. Katsumata, T. Suzuki, K. Ohta, *Chem. Eng. J.* **2007**, *128*, 47–50.

[17] S. Kaneco, Y. Ueno, H. Katsumata, T. Suzuki, K. Ohta, *Chem. Eng. J.* **2006**, *119*, 107–112.

[18] A. A. Peterson, F. Abild-Pedersen, F. studt, J. Rossmeisl, J. K. Nørskov, *Energy Environ. Sci.* **2010**, *3*, 1311–1315.

[19] C. E. Tornow, M. R. Thorson, S. Ma, A. A. Gewirth, P. J. A. Kenis, *J. Am. Chem. Soc.* **2012**, *134*, 19520–19523.

[20] E. J. Dufek, T. E. Lister, M. E. McIlwain, *Electrochem. Solid-State Lett.* **2012**, *15*, B48–B50.

[21] E. J. Dufek, T. E. Lister, S. G. Stone, M. E. McIlwain, *J. Electrochem. Soc.* **2012**, *159*, F514–F517.

[22] H. R. Jhong, F. R. Brushett, P. J. A. Kenis, *Adv. Energy Mater.* **2013**, *3*, 589–599.

[23] J. J. Wu, F. G. Risalvato, F. S. Ke, P. J. Pellechia, X. D. Zhou, *J. Electrochem. Soc.* **2012**, *159*, F353–F359.

[24] W. Z. Teo, A. Ambrosi, M. Pumera, *Electrochem. Commun.* **2013**, *28*, 51–53.

[25] R. M. Hernández, M. Kalaji, *J. Chem. Soc. Faraday Trans.* **1996**, *92*, 3957–3962.

[26] H. R. Jhong, S. Ma, P. J. A. Kenis, *Curr. Opin. Chem. Eng.* **2013**, *2*, 191–199.

[27] C. Costentin, S. Drouet, G. Passard, M. Robert, J. M. Savéant, *J. Am. Chem. Soc.* **2013**, *135*, 9023–9031.

[28] Y. P. Peng, Y. T. Yeh, S. Ismat Shah, C. P. Huang, *Appl. Catal. B* **2012**, *123*, 414–423.